Control of VINE Robots with Liquid Crystal Elastomers (LCEs)

Sukanya Krishna[1], Nicholas O'Shea[1], Alex Lu[1], Yassin Fagelnour[1], Sarah Chang[1]

***Abstract*— This paper presents an innovative control system for VINE Robots using Liquid Crystal Elastomers (LCEs), focusing on improving navigation in endovascular procedures, particularly stroke treatment. The system integrates the reversible shape-changing properties of LCEs in response to temperature variations, the heat transfer dynamics of elastic material, and the mechanics of a spring-mass damping system for precise adjustments of the robot tip position. The LCE-actuated VINE Robot, with an LCE layer on a Thermoplastic Polyurethane (TPU) body, is actuated via Nichrome wire heating. The system is modeled using Ordinary Differential Equations (ODEs), combining the relationship between thermal dynamics and mechanical motion. A tailored PID control scheme is introduced for effective actuation control, with simulations validating the robot's ability to accurately reach and maintain target positions. The study indicates significant potential for LCE-integrated VINE Robots in improving the safety and efficiency of endovascular procedures, suggesting a new direction for vascular interventions and highlighting future work on control refinement, alternative heating methods, and live imaging integration for active target positioning.**

I. INTRODUCTION

Cardiovascular diseases affect millions of people in the United States. Each year, over 795,000 individuals in the United States experience a stroke, with a significant majority—87%—being ischemic strokes characterized by the obstruction of blood flow to the brain [1].

Endovascular surgery, a minimally invasive treatment, offers a method for removing blood clots by navigating through the body's vessels. Conventional endovascular procedures typically involve using a steerable catheter, which is inserted into an artery from the arm or groin and then directed towards the blood clot under X-ray guidance [2]. Upon reaching the designated location, the procedure involves deploying a stent to ensnare and extract the clot, or alternatively, administering medication through the catheter to induce liquefaction of the clot. However, the semi-rigid nature of the catheter poses challenges, including the risk of bleeding due to blunt force or high friction as the catheter is pushed through the body. Additionally, reaching the brain requires navigating through the complex and tortuous path of the aortic arch into the carotid artery, a task made more difficult by the high variation in branch distribution, characterized by up to 11 different types [3].

Previous research has showcased the potential application of an everting Vascular Internal Navigation by Extension (VINE) robot, demonstrating its capability to navigate through vessels without introducing substantial shear force [4]. However, the need to prebend sections of the VINE during manufacturing limits its flexibility to predetermined paths. Given the intricacies of blood vessel dynamics influenced by external factors like blood flow and vessel expansion, coupled with the need to accommodate various types of aortic arches, an actively steerable VINE is necessary.

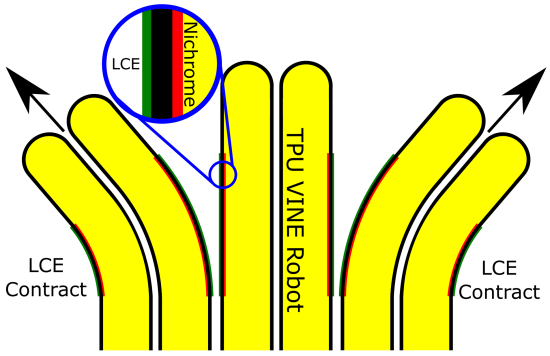

Fig. 1. The effect of LCE contraction on the bending of the VINE robot. Nichrome wires (red) are lined on the inside the TPU layer, and the LCE (green) is attached to the outside of the TPU layer.

Liquid Crystal Elastomers (LCEs), capable of contracting along one axis when heated to specific temperatures, present a promising material for achieving active steering. The LCE actuation is reversible so it will contract when heated and elongate to its original position once cooled. LCEs are constructed by layering As-spun LCE fibers, with the fabrication process capable of being changed to set the operating range to a specific temperature [5]. Further, the thickness of the LCE material can be changed in order to achieve a specific contraction force capable of bending the pressurized VINE robot [6].

By integrating a thin layer of Liquid Crystal Elastomer (LCE) onto the surface of the VINE robot, active steering could be achieved through the controlled contraction of LCE. This paper proposes a model and control scheme tailored for a VINE robot integrated with LCE, aiming to effectively control its steering capabilities.

II. METHODS

A. LCE Actuation

The LCE-actuated VINE robot will be manufactured by attaching LCE material along the exterior of the VINE robot, constructed from Thermoplastic Polyurethanes (TPU), as depicted in Figure 1. To initiate heating in the LCE, a thin Nichrome wire will be affixed to the interior of the VINE robot, and voltage will be applied across the wire to

[1]Sukanya Krishna, Nicholas O'Shea, Alex Lu, Yassin Fagelnour, and Sarah Chang are with the Department of Bioengineering, University of California, San Diego, 9500 Gilman Dr, La Jolla, CA 92092 {sskrishn, noshea, allu, yfagelno, sjchang}@ucsd.edu

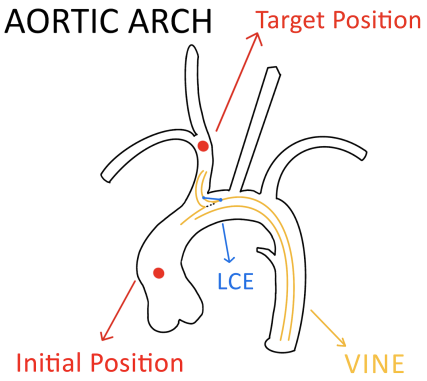

Fig. 2. A depiction of the initial and target positions within the aortic arch. The VINE body is shown in green; when the LCE contracts, the position of the VINE tip moves.

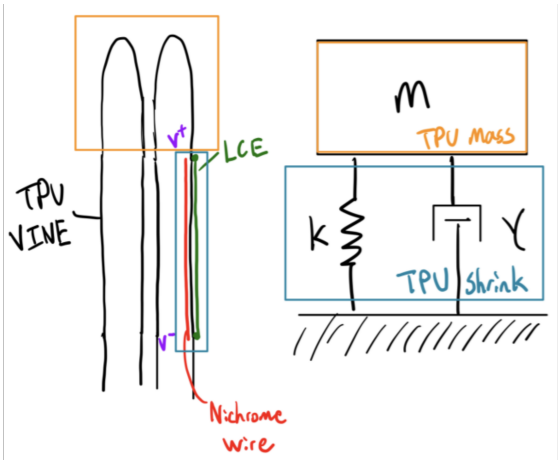

Fig. 3. The VINE as a spring-mass damping system, with the purple box highlighting the VINE body acting as the spring component, and the orange box highlighting the VINE tip acting as the mass component.

generate heating power. Once the LCE is heated, the TPU will experience a specific strain that propels the VINE robot to curve towards the actuated direction.

B. Modeling the Vine Robot

To accurately represent the LCE-actuated VINE robot in a model, it is essential to characterize the relationship between VINE bending and the operating set point, along with modeling the dynamics of Thermoplastic Polyurethane (TPU) stress-strain interactions.

1) Operating Setpoint: As the LCE undergoes heating and contraction, the segment of the VINE robot in contact with the LCE also contracts, inducing curvature. In this context, a linear relationship is established by directly correlating the strain of the VINE segment with the angulation of the VINE robot's curve. Consequently, the targeting of the VINE robot's steering is intricately linked to the shrinkage (u) generated by the LCE contraction, as displayed in Figure 2.

2) Modeling the VINE as a spring-mass damping system: The TPU material exhibits characteristics between rubber and plastic. As the LCE shrinks, it applies stress to the TPU, generating strain. The dynamics of TPU shrinkage are modeled by a mass-spring-damper system, where the elasticity of the TPU represents the spring component, the viscoelastic energy dissipation during stretching represents the damping component, and the curvature of the TPU tip represents the mass component. This modeling approach, depicted in Figure 3, is straightforward to implement and effectively captures the fundamental characteristics of the overall system.

C. Assumptions

With such a complex system, the following assumptions must be made to simplify the representation and be able to assess the modeling and control of the VINE robot.

- The amount of heat transferred to the LCE linearly affects the contraction force applied to the system.
- The damping coefficient is assumed to be 100 Ns/m, based on previous literature
- Tissue destruction occurs when the temperature exceeds 50 degrees Celsius, so we assume the temperature at which the LCEs will actuate will be in a range from $37 - 50^oC$.
- Voltage is being insulated by the TPU
- Perfect measurement of position

D. TPU Characterization and Parameters

In order for this system to be modeled, parameters within the system must be calculated, approximated, or found in literature. For TPU characterization, it is necessary to determine the mass of the TPU and its spring constant. Since the exact mass of the TPU used in the VINE robot is unknown, it must be approximated using other known characteristics, such as the thickness, circumference, and length of the TPU VINE. The thickness is 3.81×10^{-5} m, the length of the bending segment is 0.02 m, and the length ahead is 0.01 m. The volume of the outer diameter of the VINE is 5.98×10^{-9} m^3, and the volume of the inner diameter of the VINE is 4.80×10^{-9} m^3. TPU has a density of 1.28 g/cc. Using density*volume, the calculated total mass of TPU is 0.138 g.

The elastic modulus is 0.039 GPa, which is a known property of TPU. The area is 6×10^{-7} m^2 and the length is 0.02 m. Using the equation $k = \frac{AE}{L}$, the spring constant, k, of the TPU is calculated to the 1170 N/m.

Since the VINE robot will operate within the heart, where blood is always flowing, the temperature applied to the LCE will not be representative of the actual temperature of the LCE because the flow of blood will take heat away from the system. Using the following equation [7]:

$$h = \frac{\rho c u (T_1 - T_0) b}{[0.25(2T_s + T_1 + T_0) - T_m]a} \quad (1)$$

The heat transfer coefficient for blood flow can be calculated to account for this heat loss. Using the parameters in Table 1, the heat transfer coefficient for blood flow is h = 0.0103 W/K

TABLE I

HEAT TRANSFER COEFFICIENT PARAMETERS

Symbol	SI Values
ρ (blood density)	1000 kg/m^3
c (blood specific heat)	4180 J/kg*K
u (mean blood velocity)	0.18 m/s
T_0 (inlet temp.)	37^oC
T_1 (outlet temp.)	37.05^oC
T (max temp.)	50^oC
T (medium temp.)	37.024^oC
a (length of the heated region)	0.02 m
b (diameter of the heated region)	0.0049 m

E. System of Ordinary Differential Equations (ODEs)

In our comprehensive system model, using the parameters in Table II, the primary focus is on the key dynamics governing a soft VINE robot with embedded liquid crystal elastomer (LCE) actuators. The system is governed by a set of three interconnected equations representing the heating dynamics, motion dynamics, and LCE contraction dynamics.

$$m_{LCE}c_{LCE}\frac{dT}{dt} = \alpha P - h_{bl}(T - T_{bl}) \tag{2}$$

$$m_{TPU}\frac{dv}{dt} = -ku - \gamma v + \beta(\frac{T - T_{low}}{T_{high} - T_{low}}) \tag{3}$$

$$\frac{du}{dt} = v \tag{4}$$

TABLE II

PARAMETER VALUES

Symbol	SI Values	Source
c_{LCE}	1570 J/kg·K	LCE specific heat
V_{LCE}	1.2×10^{-7} m^3	Volume
m_{LCE}	1.5×10^{-4} kg	Volume×Density
h_{bl}	0.0103 W/K	H.T. Model
k	1170 Ns/m	TPU Spring
γ	100 Ns/m	Assumption
m_{TPU}	0.000138 kg	Thin film TPU density
T_{bl}	310.15 K	Body temperature
T_{low}	310.15 K	LCE operating point
T_{high}	323.15 K	LCE operating point
β	23.4 N	LCE manufacturing
α	0.0000537	Power coefficient

Equation 2 captures the heating dynamics of the LCE actuators, modeling the temperature change resulting from the input power, where heat dissipation is assumed to predominantly be influenced by blood flow. This temperature change, a crucial parameter in the system, is directly related to the force at which the LCE actuators contract, forming one of the inputs for Equation 3. Modeled as a Newtonian dynamics equation, this third equation describes the motion of the VINE, treating the soft robot as a spring-mass-damper system. Subsequently, the VINE's velocity is derived from this dynamics equation, establishing a direct relationship with its position, as outlined in Equation 4. These equations provide a comprehensive framework to understand and analyze the complex interactions between thermal dynamics, mechanical motion, and LCE actuation within the soft VINE robot system.

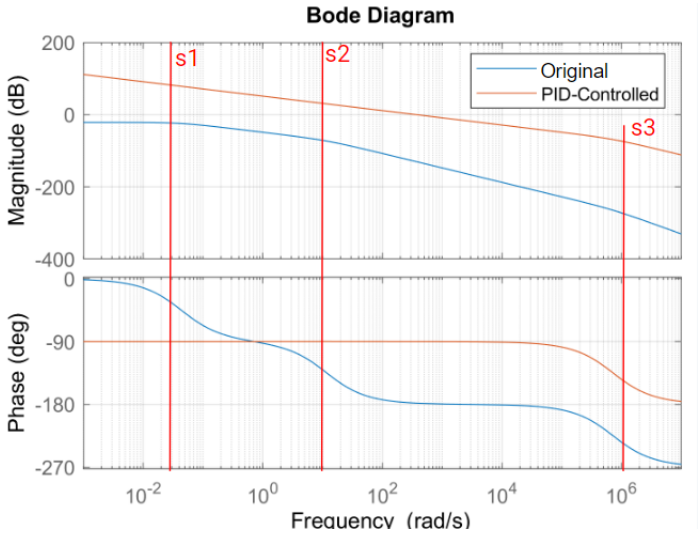

Fig. 4. Bode Plot for Transfer Function with (orange) and without (cyan) PID Control. The first (s1), second (s2), and third (s3) poles of the system are indicated in red.

III. RESULTS

A. Transfer Function, Bode Plot, and PID Control

With power as input and shrink position as output, a transfer function, can be derived via the LaPlace transform of the ODEs.

$$\frac{u(s)}{P(s)} = \frac{\alpha\beta}{(T_{high}-T_{low})(m_{LCE}c_{LCE}s+h_{bl})(m_{TPU}s^2+\gamma s+k)} \tag{5}$$

From the transfer function, presented in Equation 5, the poles of the system were discovered, and a bode plot was constructed in MATLAB. As seen in Figure 4, the original Bode Plot indicates horrible bandwidth, negative DC gain, and up to -270° phase. It is clear that incorporating a Proportional-Integral-Derivative (PID) control for the system would be ideal.

First, the proportional component directly lifts magnitude to improve the phase margin. The integral component, situated at the first pole, ensures infinite gain at DC, reducing DC error. The derivative component at the second pole enhances the system's phase margin by lifting the phase at higher frequencies. Because the third pole occurs at a very high frequency, the effect of that pole on the system can be neglected.

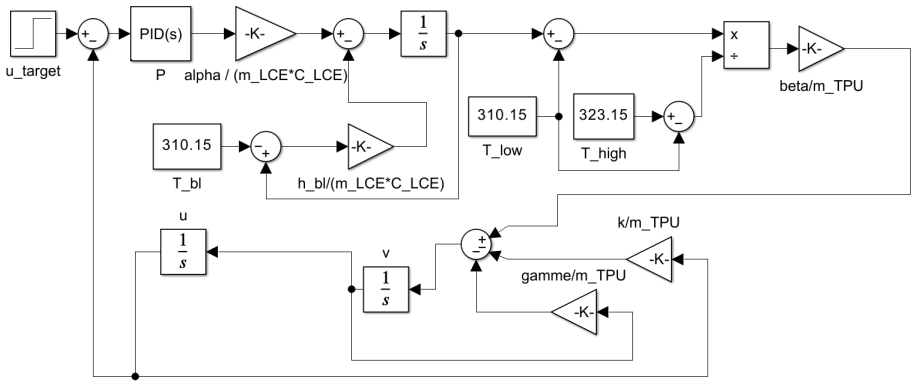

Fig. 5. Block Diagram to simulate power and position response of soft VINE robot system

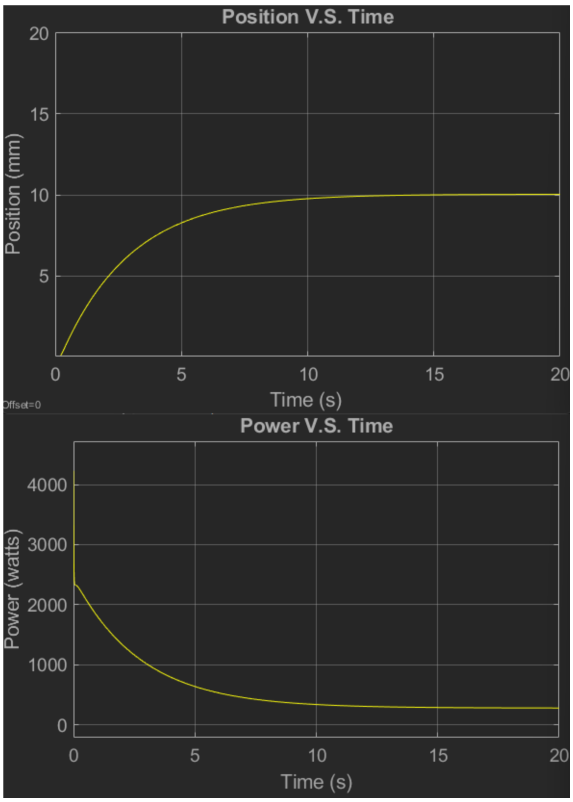

Fig. 6. Power and position responses with single input position

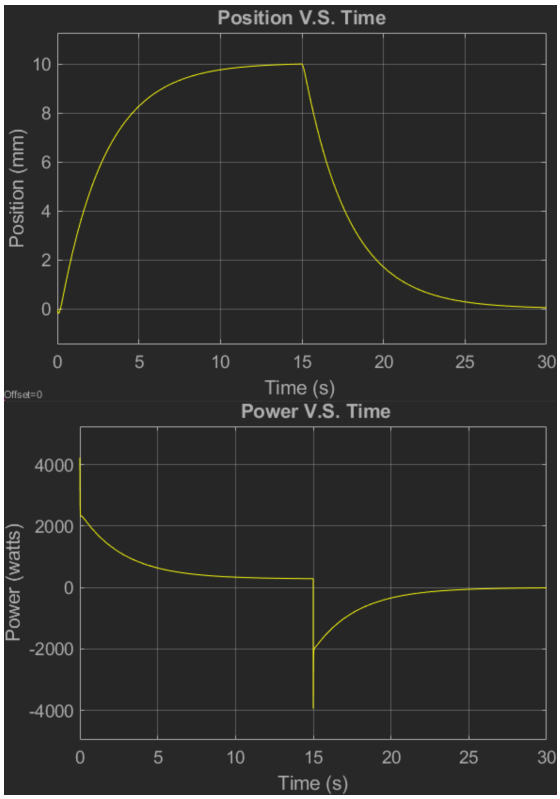

Fig. 7. Power and position responses with two input positions separated by a delay

The PID controller is characterized by tuning parameters: $\frac{K_I}{K_P}$ = 0.0437 and $\frac{K_P}{K_D}$ = 11.702, with specific values of K_P = 100000, K_I = 4370, and K_D = 8545. The resulting system features a bandwidth of 370 rad/s and a phase margin of 90 degrees, displayed in Figure 4, embodying a well-tailored PID control strategy for effective regulation and stability in the soft VINE robot's dynamic response.

B. Overall Block Diagram

A block diagram representing all of the components of the biosystem was generated in Simulink (Figure 5). The power input is modeled as a step function and will be controlled via a PID controller whose input is the difference between the target and the current position of the VINE robot.

C. Single and Double Input Responses

By setting the initial conditions and inputting a target value, the control system can simulate the movement of the VINE as it adjusts from its current to the target position while taking into account the dynamics of the system. The model is first tested by inputting a target position of $u_t = 10$, causing the VINE tip to move from its initial position of u = 0. The dynamics of the system are simulated using the Simulink block diagram. As shown in Fig 6, the power is initially increased to cause the LCE to heat and actuate, which moves

the VINE tip from u = 0 to u = 9 in just 5 seconds, then power decreases as the position steadily reaches the target value of u = 10 in an additional 5 seconds. Second, the system is tested by changing the target position at t = 20 seconds to model how the control system works with a changing target position. This is done by first setting the target position to u = 10 and then changing the target position to u = 0 which models both the LCE actuation and relaxation. In Fig 7, the power is initially high until the position reaches its target as in the single input response, but after the target is changed to u = 0, the power drops rapidly causing the LCE to cool off and return to its original shape, resulting in the VINE to move to its desired position of u = 0. The negative power represents the actuation of LCE in the opposite direction.

IV. Discussion

A. Advantages

With our proposed model and control system for the VINE robot integrated with LCE, the contraction of the LCE will be effectively controlled, enhancing its steering and navigation capabilities. This control system can lead to a potential for improved patient outcomes. Unlike current conventional procedures, the active steering capability of the VINE robots minimizes shear force, which would reduce the risks associated with traditional endovascular procedures, such as bleeding. Additionally, the VINE allows for more adaptation to different anatomies and the various needs of specific procedures. This ability to navigate through vessels without causing substantial shear force enhances the safety and effectiveness of endovascular procedures.

While initially being designed to navigate the body's vessels to clear blood clots and treat strokes, the VINE robot is extremely versatile and can be used for a wide range of surgical applications. One significant application is using it as a way to improve angioplasties by providing a more effective method of delivering stents to the coronary arteries. This can mitigate the risks of coronary artery damage and bleeding that is associated with current angioplasty techniques, enhancing the safety of the procedure. Additionally, the VINE's enhanced steering and navigation capabilities can also be used for more precise medicine injection or other treatments during surgical procedures, such as atrial fibrillation treatment. The current leading treatment for atrial fibrillation is ablation, where heat or cold energy is used to target and "burn" cells causing irregular electrical signals [8]. This comes with the risk of blood vessel or heart valve damage, which can be mitigated by controlling the device more precisely with the VINE robot.

B. Potential Sources of Error

In this report, we aim to model movement through a complicated biosystem by simplifying models and limiting assumptions. In any case, many potential sources of error are a result of these simplifications. First, the assumption that there is a linear relationship between the amount of heat transferred and the rate of curving does not hold in a real-world VINE. This is because the LCE does not contract evenly based on the temperature in its working range, but rather reaches a critical temperature within the anisotropic fibers in which they align and cause a larger contraction in the center of the working range than the extremes. Further, the strain exerted on the VINE from the LCE is also not directly proportional to the bending because there is a minimum force that must be overcome to start the movement of the VINE as it is held at a constant pressure to grow. Additionally, because the VINE body curves in a circular fashion, the initial curving will be greater for the same amount of actuation than the curving happening as it is already bent and further along in its circular trajectory. However, since simplifications of the linear relationship of both heating and bending from strain give an overestimate of the curving and the simplification of the circular path underestimates the movement of the VINE; these errors may partly cancel each other out and the total error will be small. In comparison with the speed of the control system, these errors do not significantly hinder the performance of the feedback system.

Another source of error comes from the calculation and estimation of the alpha, beta, and damping coefficient values as they were based on previous literature which may differ slightly from our specific application. This may cause a discrepancy between the behavior of our system and the actual behavior of the physiological system within the body.

C. Limitations

A larger source of error may be in the physical limitations and time-varying properties of the soft robot. For example, we assume heating occurs instantaneously, but there is likely a significant time delay between the activation of the heated wire and the increase in temperature of the LCE. This may cause the PID controller to over (or under) heat the wire as it assumes heating occurs instantaneously, even though the temperature has not increased; this forces a higher power output and eventually a wire that has too much current flowing through it. Similarly, the model does not account for latent heat in the LCE and assumes cooling from diffusion and convection from the surrounding blood flow occurs instantaneously. This would likewise cause the PID controller to incorrectly assume there should be an even greater decrease in current in the wire and cause an underestimate in the position of the VINE. In future work, more complex time-varying properties such as these will need to be included to create a more accurate biosystem.

In addition to the sources of error listed, other limitations are beyond the scope of the simplified biosystem described in the report. For example, during endovascular surgery, the heart is continually pumping blood through the large arteries connected to the heart. So, to fully describe the system, the complex fluid dynamics of the circulatory system must be taken into account. Another factor that is not fully described in the model is the variations in temperature both within the VINE and the surrounding environment. For example, we assume heating occurs uniformly across the VINE and LCE but in reality, there may be sections that are hotter

or colder than others and thus exhibit different properties and characteristics. Further, some organs may have differing temperatures or heat transfer coefficients causing an even greater increase in temperature variation.

D. LCE Considerations

Limitations of LCE manufacturing include limits to maximum strain, a time intensive process, and unknown reproducibility. Since the LCEs are limited in their maximum strain, there is a limit on the minimum bending radius; however, this will not exceed the bending radius needed to navigate the aortic arch. For manufacturing, the process will need to be automated in future work for this to be viable in commercial settings. Also, unknown reporducibility of the LCE may cause differences between the expected strain in the model and the observed strain in the body resulting in a larger observed error in position.

E. Alternative Heating Methods

One major concern of the workability of the soft robot is the method of heating the LCE by use of wire. Since a voltage is being applied to a wire that conducts a current throughout the length of the VINE which is in the body there is a risk of breakage and electric shock. Since TPU is an insulator, we assume the wire is fully insulated from the surrounding environment, and due to minimal shear forces damage to the VINE is unlikely; however, if there is a tear or breakage, high levels of voltage may be exposed and cause the body to be electrocuted. To find an alternative method that allows the voltage to decrease, we have considered using different conductive materials such as nichrome in addition to copper as well as conductive paste, laser-cut copper sheets, and sputtered metals to decrease the required voltage and current to reach activation temperatures.

Other non-invasive methods are likely to be considered when deciding how to properly heat the LCE. One method involves the use of electromagnetic induction to transfer current from an external source placed on the skin which induces a current on a metal coating on either the LCE or TPU [9]. This allows heating to occur which enters the body by the use of an electromagnetic field. Similarly, an ultrasound can be used to probe the body with ultrasonic waves which cause particles to vibrate and create heat. Ultrasound is commonly used in cosmetic surgery involving fat tightening procedures which involve heating the fat cells to temperatures above 50 degrees Celsius and cancer treatment which focuses ultrasonic waves onto the affected area and heating unwanted cancer cells. This is also useful as the frequency can be tuned to reach a certain depth which can correspond to the depth at which the LCE is found [10]. Further, gold or magnetic nanoparticles can be added to the fabrication of the LCE material to increase the temperature and locality of the heating of the LCE [11] [12]. So, both of the methods can be used to non-invasively heat the LCE without severely limiting the response time of the control loop system. However, these are yet to be tested and will need further verification for widespread adoption.

Lastly, the use of pumping hot water or PBS into the VINE is a highly biocompatible solution that can be used if the time-varying response of the temperature is properly accounted for in the model. Since the VINE will already need to be inflated with water or PBS solution to both evert the VINE and provide sufficient pressure and properties of the existing arteries (air may cause damage if leaked), all that would have to be done is change the temperature of fluid entering the VINE assuming it will reach the end of the VINE in a short time period. This is likely the most simple approach and useful if the actuation of the VINE occurs in one direction.

F. Active Target Positioning

One of the primary motivations of the biosystem is to create a control loop that can accurately move the tip of the VINE to a specified position corresponding to the beginning of the carotid artery. In our model, we modeled the response to move to both a single position as well as a second position in which the control system was able to change direction and steer to the new target position. In a real-world scenario, the target position will not be stationary as the heart moves every time it pumps for each heartbeat as well as shift in position as the body itself moves voluntarily and involuntarily. So, it is crucial that a working control system can actively steer the tip of the VINE to an actively moving target position as the eversion takes place. This was not introduced in this paper due to the complexity and lack of a systematic way to measure the position of the stated artery. However, with modern technology and advanced imaging techniques, a live map of the updated position can continually be fed to the PID controller which can actively adjust to the desired location. In future work, the live imaging map of the arteries can be connected to the model; this allows the active target positioning to be incorporated into the control system which will provide an accurate control of the desired position during surgery.

V. Acknowledgements

We would like to thank Professor Cauwenberghs and Teaching Assistant Benjamin Balster for all their help this quarter.

References

[1] Centers for Disease Control and Prevention (CDC), "Stroke facts — cdc.gov." https://www.cdc.gov/stroke/facts.htm, Sep 2023. Accessed: 2023-09-06.

[2] Cardiovascular and Interventional Radiological Society of Europe (CIRSE), "Endovascular treatment of stroke." https://www.cirse.org/patients/general-information/ir-procedures/endovascular-treatment-of-stroke/, 2023. Accessed: 2023-12-14.

[3] Medwave.cl, "Anatomic variations of the branches of the aortic arch in a peruvian population," Section: Research papers.

[4] M. Li, R. Obregon, J. J. Heit, A. Norbash, E. W. Hawkes, and T. K. Morimoto, "VINE catheter for endovascular surgery," vol. 3, no. 2, pp. 384–391.

[5] Q. He *et al.*, "Electrospun liquid crystal elastomer microfiber actuator," *Science Robotics*, vol. 6, p. eabi9704, Aug 2021.

[6] Q. He *et al.*, "Electrically controlled liquid crystal elastomer–based soft tubular actuator with multimodal actuation," *Science Advances*, vol. 5, p. eaax5746, Oct 2019.

[7] I. dos Santos, D. Haemmerich, C. d. S. Pinheiro, and A. F. da Rocha, "Effect of variable heat transfer coefficient on tissue temperature next to a large vessel during radiofrequency tumor ablation," vol. 7, p. 21.
[8] M. Clinic, "Cardiac ablation," 2022. Mayo Foundation for Medical Education and Research.
[9] "High intensity focused ultrasound (hifu)." https://www.cancerresearchuk.org/about-cancer/treatment/other/high-intensity-focused-ultrasound-hifu, 2023. Accessed: Dec. 14, 2023.
[10] S. Mortazavi and M. Mokhtari-Dizaji, "Numerical study of high-intensity focused ultrasound (hifu) in fat reduction," *Skin Research and Technology*, vol. 29, p. e13280, Jan 2023.
[11] S. B. Devarakonda *et al.*, "Assessment of gold nanoparticle-mediated-enhanced hyperthermia using mr-guided high-intensity focused ultrasound ablation procedure," *Nano Letters*, vol. 17, pp. 2532–2538, Apr 2017.
[12] K. Kaczmarek *et al.*, "Influence of magnetic nanoparticles on the focused ultrasound hyperthermia," *Materials*, vol. 11, p. 1607, Sep 2018.